AMEGHINIANA
A GONDWANAN PALEONTOLOGICAL JOURNAL

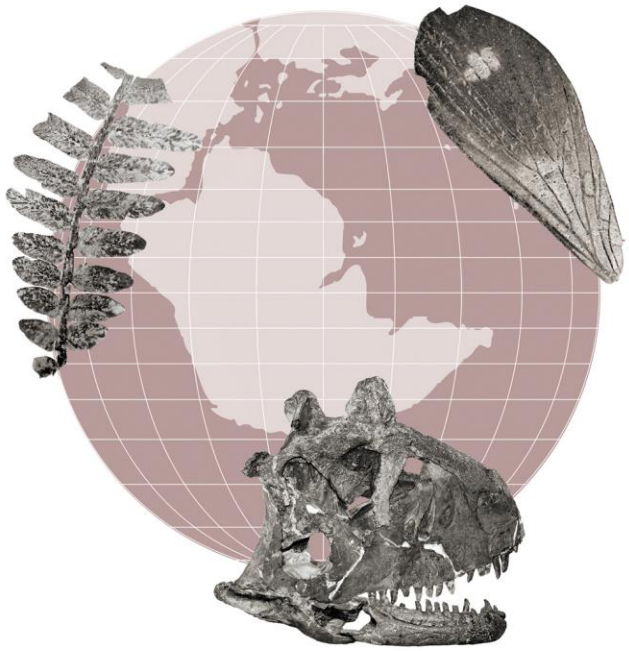

Submitted: 16 July 2025 - **Accepted**: 26 November 2025 - **Posted online**: 30 November 2025

To link and cite this article:

doi: 10.5710/AMGH.26.11.2025.3659

PLEASE SCROLL DOWN FOR ARTICLE

COMPLETENESS, CONVERGENT MORPHOLOGY AND POSITIVE NARRATIVES: AN INTRIGUING SNAKE SKULL FROM THE MIDDLE-LATE EOCENE OF ARGENTINA

AGUSTÍN SCANFERLA[1,2], JUDITH BABOT [1,3], AND DANIEL GARCÍA LOPEZ[1,4,5]

[1]Consejo Nacional de Investigaciones Científicas y Técnicas (CONICET)

[2]Fundación de Historia Natural "Félix de Azara" Centro de Ciencias Naturales, Ambientales y Antropológicas, Universidad Maimónides, Hidalgo 775, C1405BCK, Ciudad Autónoma de Buenos Aires, Argentina. agustinscanferla@yahoo.com.ar

[3]Fundación Miguel Lillo-Unidad Ejecutora Lillo (UEL-CONICET), Miguel Lillo 251, 4000, San Miguel de Tucumán, Tucumán, Argentina. mjbabot@lillo.org.ar

[4]Instituto Superior de Correlación Geológica (INSUGEO), Universidad Nacional de Tucumán (UNT). Avenida Presidente Perón S/N, 4107 Yerba Buena, Tucumán, Argentina. dgarcialopez@csnat.unt.edu.ar

[5]Facultad de Ciencias Naturales e Instituto Miguel Lillo, Universidad Nacional de Tucumán (UNT). Miguel Lillo 205, 4000 San Miguel de Tucumán, Tucumán, Argentina.

38 pag. (text + references); 7 figs.

Short Description: We describe and discuss an intriguing fragmentary skull of an Eocene snake from Argentina.

26 Corresponding author: Agustín Scanferla-agustinscanferla@yahoo.com.ar

Abstract. We describe a partial snake neurocranium recovered from Eocene levels of the Geste Formation (Catamarca, Argentina). Preserved bones are fused, and the otic capsules are relatively enormous with a large stapedial footplate closing the fenestra ovalis. µCT imagery allows the recognition of a fenestra pseudorotunda that communicates the vestibular cavity with the juxstastapedial recess, and the occipital condyle is rounded (i.e. fovea dentis absent). This unusual combination of features known elsewhere only in uropeltid snakes, a group of Indian and Sri Lankan basal alethinophidians related with other Indomalayan snakes that together comprise the clade Uropeltoidea. A thorough anatomical analysis of skull of cryptozoic and surface-dwelling miniaturized colubroideans demonstrates that a fenestra pseudorotunda and the fusion of neurocranial bones are also present in other ophidian clades, thus questioning the diagnostic value of these features. A combined phylogenetic analysis (morphology plus DNA) places this fossil specimen as an uropeltoid. If new and more complete specimens confirm this result, Indomalayan uropeltoid snakes represent a biogeographic puzzle that implies its probable origin in a Gondwanan terrain and a dispersion to peninsular India, Sri Lanka and South East Asia between the Late Cretaceous to the Paleogene. However, the fragmentary nature of the specimen and the pervasive morphological convergence observed among burrowing and surface-dwelling miniaturized snakes suggest that caution is warranted. Pressure upon scientists to boost their publication output in high-ranked journals can potentially lead to the elaboration of attractive, positive narratives about complex evolutionary and paleobiogeographic scenarios, even when based on fragmentary specimens. Due to the often limited informativeness of fragmentary specimens, such evolutionary hypotheses are often weakly supported and thus can complicate instead of benefit the advancement of our knowledge of ophidian evolution.

Keywords. Geste Formation. Late Eocene. Argentina. Snake neurocranium. Uropeltoidea. Positive narratives.

Resúmen. COMPLETITUD, CONVERGENCIA MORFOLÓGICA Y NARRATIVAS POSITIVAS: UN INTRIGANTE CRÁNEO DE SERPIENTE DEL EOCENO MEDIO-TARDÍO DE ARGENTINA. Describimos un neurocráneo incompleto de serpiente hallado en niveles del Eoceno de la Formación Geste (Catamarca, Argentina). Los huesos conservados del espécimen fósil están fusionados y las cápsulas óticas son enormes, con un gran pié columelar obturando la fenestra ovalis. Las imágenes de µCT permiten reconocer una fenestra pseudorotunda que comunica la cavidad vestibular con el receso yuxstastapedial, y el cóndilo occipital es redondeado (i.e. fovea dentis ausente). Esta inusual combinación de rasgos sólo es conocida en uropeltidos, un grupo de aletinofidios basales emparentados con otras serpientes de la region Indomalaya que conforman el clado Uropeltoidea. Un minucioso análisis anatómico del cráneo de colubroideos miniaturizados criptozoicos y de superficie demuestra que la fusión de los huesos neurocraneales y la fenestra pseudorotunda también están presentes en otros grupos de serpientes, lo que cuestiona el valor diagnóstico de estos rasgos. El análisis filogenético de evidencia combinada sitúa este espécimen fósil como un uropeltoideo. Si esta relación filética se confirma con nuevos ejemplares más completos, los uropeltoideos Indomalayos representan un rompecabezas biogeográfico que implica su probable origen en un terreno gondwánico y una dispersión a la India peninsular, Sri Lanka y el Sudeste Asiático entre el Cretácico Superior y el Paleógeno. Sin embargo, el carácter incompleto del espécímen y la convergencia morfológica observada entre las serpientes miniaturizadas fosoriales y de superficie invitan a ser cautos. La creciente presión sobre los científicos para aumentar su producción de publicaciones en revistas

de alto rango a menudo conduce a la elaboración de narrativas atractivas y positivas sobre complejos escenarios evolutivos y paleobiogeográficos basados en especímenes fragmentarios. Debido a la reducida información que proveen los especímenes fragmentarios, estas hipótesis evolutivas podrían estar escasamente sustentadas, representando así un paso atrás que complica en lugar de beneficiar el avance de nuestro conocimiento sobre la evolución de los ofidios.

Palabras clave. Formación Geste. Eoceno superior. Argentina. Serpiente. Neurocráneo. Uropeltoidea. Narrativas positivas.

THE REVOLUTION of snake systematics ignited by the molecular phylogenies has been key in our awareness that biomechanical challenges exerted by the life underground led similar transformations in the skull in distantly related clades of ophidian. Convergence thus represents a pervasive phenomenon in the skeleton among fossorial and cryptozoic snakes (Savitsky, 1983; Lee, 1998; Miralles *et al*., 2018; Strong *et al*., 2021a, 2021b).

One of the phylogenetic signals provided by molecular analyses that changed the traditional snake tree is the paraphyly of "Anilioidea", a clade of fossorial and cryptozoic snakes traditionally recognized through morphological features that included the Amazonian false coral snake *Anilius scytale* and the uropeltoid snakes. Based both in morphology and DNA data, Uropeltoidea is a well-established monophyletic group formed by species of the genera *Cylindrophis*, *Anomochilus* and the shieldtail snakes (Uropeltidae), all currently distributed in the peninsular India, Sri Lanka and South East Asia. The fossil record of these early-diverging alethinophidians is notably scant, counting only with some isolated skull elements and vertebrae probably related with *Anilius scytale* more than uropeltoids (Rage, 1974; Gómez et al., 2008; Head, 2021). Therefore, new systematic arrangements plus the fragmentary nature of its fossil record have discloced our incomplete and sometimes contradictory picture about "anilioid" evolution, especially expressed in the independent acquisition of osteological traits with strong ties to underground life.

Paleogene sedimentary units of Northwestern Argentina have yielded few snake specimens of relatively large size forms belonging to "macrostomatans" and extinct groups such as "madtsoids" (Albino, 2018; Garberoglio *et al.*, 2022). Recent fieldwork in late Eocene levels of the Geste Formation resulted in the finding of a fragmentary neurocranium of a small snake, together with a rich vertebrate fauna conformed by

anurans, lizards and mammals (López, 1997; Reguero *et al*., 2008; García-López & Babot, 2015; Ciancio *et al*., 2016; Babot *et al*., 2018, 2019; Gómez *et al.*, 2025). This fragmentary snake specimen clearly exhibits an intriguing combination of features observed among different burrowing alethinophidian snakes, including "anilioids". Hence, the aim of this contribution is to describe the morphology and explore the phylogenetic relationships of this fossil specimen through a thorough anatomical and phylogenetic analysis, and thus to discuss the relevance of a suite of cranial traits present in burrowing extant snakes.

Institutional abbreviations. CAS, California Academy of Sciences, San Francisco, USA; **FMNH,** Field Museum of Natural History, Chicago, USA; **INPA,** Instituto Nacional de Pesquisas da Amazônia, Manaus, Brazil; **KU**, Kansas University Biodiversity Institute, Lawrence, USA. **MCZ,** Museum of Comparative Zoology, Cambridge, USA.; **MHAS**, Museo del Hombre de Antofagasta de la Sierra, Catamarca, Argentina; **RMNH,** Rijksmuseum van Natuurlijke Historie, Leiden, Netherlands; **UMMZ,** University of Michigan Museum of Zoology, Ann Arbor, USA.

Anatomical abbreviations. aa, anterior ampulla; **af,** foramen for the passage of the acoustic (VIII) nerve; **ap,** alary process of the prootic; **apl,** apertura lateralis recessus scalae tympani; **as,** anterior semicircular canal; **bo**, basioccipital; **c,** occipital condyle; **cb,** compound bone; **cc,** crus communis; **cp,** condylar process of the otooccipital; **ct,** crista tuberalis; **d,** dentary; **ec,** ectopterygoid; **fd,** fovea dentis; **fp,** foramen perilymphaticum; **jf,** jugular foramen; **ls,** lateral semicircular canal; **mx,** maxilla; **oc,** occipital complex; **ot,** otooccipital; **p,** parietal; **pa,** palatine; **pbs,** parabasisphenoid; **pot,** prootic; **ps,** posterior semicircular canal; **pt,** pterygoid; **q,** quadrate; **qc**, cephalic condyle of the quadrate; **s,** stapedial footplate; **sg,** sagittal crest of the basioccipital; **so,**

supraoccipital; **ss,** base of the stapedial shaft; **ssf,** fossa that receives the tip of the suprastapedial process of the quadrate; **st,** supratemporal; **stf,** surface of contact with supratemporal?; **v,** vestibulum; **V_2,** foramen for the passage of the maxillary ramus of the trigeminal nerve; **V_3,** foramen for the passage of the mandibular ramus of the trigeminal nerve; **VII,** foramen for the passage of the hyomandibular ramus of the facial nerve; **XII,** foramina for the passage of the hypoglossal nerve.

Geological Setting

Specimen **MHAS** 087 was found in fine-to-medium micaceous reddish sandstones intercalated with coarse conglomerate-sandstone matrix and subordinate mudstone, corresponding with the middle member of Geste Formation that crops out at Antofagasta de la Sierra (Catamarca, Argentina). Levels were probably deposited in a braided, high-energy fluvial system with minor floodplains in a warm subtropical or tropical seasonally dry to humid environment (DeCelles *et al.*, 2007; Ciancio *et al.* 2016; Ledesma *et al.*, 2019). A recently documented fossil assemblage comprising possible brachycephaloid, odontophrynid, and hemiphractid anurans suggests the existence of humid forests in the middle member of the Geste Formation at this locality, similar to current-day Austral Yungas and the Atlantic Forest (Gómez *et al.*, 2025).

MATERIAL AND METHODS

µCT data

Specimen MHAS 087 was scanned using micro-computed tomography on a TomoScope HV 500 (Werth Messtechnik, GmbH) in an industrial µCT facility funded by the Wolfgang Pfeiffer Stiftung at the Technische Hochschule in Deggendorf, Germany. The scan parameters were: 150 mA, 165 kV, 1600 steps, no binning or drift

correction, voxel resolution 12.68 µm. The volume files were analyzed using VG Studio MAX v3.2 on a high-end computer workstation at Senckenberg Gesellschaft für Naturforschung (Frankfurt am Main, Germany). We digitally prepared the specimen, virtually removing the matrix to expose internal structures of the neurocranium. Also, we segmented the stapes in order to observe the structure of the inner ear.

In order to assess the influence of miniaturization and/or burrowing in skull anatomy we made a thorough anatomical comparative analysis in a suite of features present in neurocranium and suspensorium across several colubroidean species previously recognized as burrowers and/or miniaturized surface-dwelling forms (see Appendix). Hence, dry skeletons and µCT data of several cryptozoic and fossorial alethinophidian snake species was gathered (see Appendix). Some of the µCT scans were generated in the Laboratorio Argentino de Haces de Neutrones (LAHN, CNEA), the rest were downloaded from MorphoSource. The set of characters includes the neurocranial conformation, ear anatomy, suspensorium and the occipital condyle, all traits prone to be convergently acquired in burrowing snakes (Savitsky, 1983; Cundall & Rossman, 1993; Lee, 1998; Strong *et al*., 2021a, 2021b).

Phylogenetic analysis

In order to test the phylogenetic relationships of the new specimen, we performed a combined (morphology + DNA) phylogenetic analysis. The matrix was assembled in Mesquite v.2.6 (Maddison & Maddison, 2007). The morphological matrix of Scanferla *et al.* (2016) was modified slightly for this purpose, including the addition of the uropeltid *Melanophidium wynaudense* (sister group of all other uropeltids) and eight additional characters obtained from the literature (Rieppel & Zaher, 2002; Olori & Bell, 2012; see online supporting information) and personal observations (available at

MorphoBank, http://morphobank.org/permalink/?P5863). The morphological matrix was combined with DNA sequences for three mitochondrial (12S, 16S, Cytb) and five nuclear genes (BDNF, Cmos, PNN, NGFB, NTF3), all taken from the GenBank (see online supporting information). The choice of these particular genes corresponds with their availability in GenBank for selected terminals in order to reduce the amount of missing data. If multiple sequences were available in GenBank for a given taxon, we selected only one sequence and chose the most complete sequence for inclusion. We employed static homology via multiple alignment using default settings in Clustal X (Thompson *et al.*, 1997). After alignment, each sequence was trimmed of its leading and lagging gaps using the program Bioedit (Hall, 1999). The lengths of the DNA sequences in base pairs and gaps were: (356) 12S, (440) 16S, (1119) Cytb, (670) BDNF, (573) Cmos, (579) NGFB, and (945) PNN. Thus, the resulting combined matrix counts with 5369 characters scored for 39 terminals (available at MorphoBank, http://morphobank.org/permalink/?P5863).

The combined matrix was analyzed in TNT (Goloboff & Morales, 2023) with all characters treated as unordered and gaps coded as missing data. The general analytical method employed was maximum parsimony (Farris, 1983). The search strategy employed in TNT was “Traditional search” (using TBR) with 1000 replications with the objective of encountering all possible tree islands. Two alternative support measures (Bremer support and bootstrap resampling) were obtained with TNT to evaluate the robustness of the nodes of the most parsimonious trees. Bootstrap values were calculated with 1000 pseudoreplicates. The trees were rooted utilizing the anguimorph lizard *Varanus salvator* as outgroup, based on proposed anguimorph-snake relationships (Forstner *et al.*, 1995; Vidal & Hedges, 2005; Streicher & Wiens, 2017).

RESULTS

Anatomical description

The specimen **MHAS** 087 consists of an incomplete, partially eroded neurocranium including both otic regions, both stapedial footplates and the posterior part of the basicranium (Fig. 1.2). Preserved bony elements are fused as in most uropeltid snakes except *Melanophidium* species (Cundall & Irish, 2008; Rieppel & Zaher, 2002; Olori & Bell, 2012; Fig. 2).

In general aspect the specimen exhibits the typical configuration present in burrowing snakes such as "anilioid" snakes (*Anilius scytale* plus Uropeltoidea), with sizeable otic capsules and a massive stapedial footplate as the most noteworthy features (Fig. 2.1, 2.2, 2.6). The preserved portion of the basicranium corresponds with the basioccipital, which shows a concave ventral shape divided longitudinally by a strong sagittal crest evidenced by its preserved broad base (Fig. 2.6). Among uropeltoids (cylindrophiids, *Anomochilus* species and Uropeltidae) only cylindrophiids bear a sagittal crest in the basioccipital (Fig. 3.5, 3.6), whereas the basioccipital of uropeltids exhibits a smooth convex surface (Fig. 3.3, 3.4). The occipital condyle is spherical due to the absence of an indentation (fovea dentis of Williams [1959]) on the dorsal surface of the condyle (Fig. 2.4). The absence of the fovea dentis leaves the occipital condyle almost spherical, as in uropeltids (Fig. 3.3, 3.4), which is connected to the neurocranium in MHAS 087 via a short stalk as in the early-branching uropeltids *Melanophidium* (Fig. 3.3) and *Teretrurus* (Fig. 3.4). There is no sign of suture or notch in the dorsal surface of the otic region for the attachment of the supratemporal, although a rugose surface in the lateroposterior region of the dorsal surface of the otic capsules (Fig. 2.1, 2.5) suggests the presence of a splint-like reduced supratemporal as in *Anomochilus weberi* (but not in *A. leonardi* [Rieppel & Maisano, 2007)]) and other miniaturized snakes that

exhibit a marked reduction of the supratemporal bone. Due to the strong reduction or absence of the supratemporal, we infer that the cephalic condyle of the quadrate contacted directly, at least in part, the neurocranium as in uropeltids (Fig. 3.3, 3.4), more precisely with the dorsolateral edge of the prootic just above the large fenestra ovalis (Fig. 3.1). This interpretation is in concordance with the presence of a small fossa in the posterior sector of this edge, as in uropeltids (Fig. 3.3, 3.4) which receives the posterior tip of the elongated suprastapedial process of the quadrate bone that characterizes the suspensorium of these snakes (Olori & Bell, 2012).

Sizeable otic capsules are nearly in contact in the skull roof of MHAS 087 (Fig. 2.3). Both stapedial footplates are preserved, but they are dislocated and only the right bears the base of the stapedial shaft (Fig. 2, 4.1). The posterior region of the stapedial footplate bears an expanded facet that contact the prootic bone in the same fashion as in other burrowing snakes. Despite the stapedial shaft is broken in the right stapes, the preserved portion indicates a broad base (Fig. 4.1, 4.2). The crista circumfenestralis, which in snakes delimits the juxtastapedial recess, is eroded in its ventral aspect (Fig. 2.6, 3.1, 3.2). Only a small piece of the crista tuberalis can be seen in the left side, which exhibits a similar relation with the jugular foramen as in uropeltoids (Fig. 3.3, 3.4, 3.5, 3.6). There are two hypoglossal foramina as in *Melanophidium* and cylindrophiids (Fig. 3.1), in contrast with the single, enlarged hypoglossal foramen present in most uropeltids (Fig. 3.3, 3.4).

The anatomy of the ear is very particular. A fenestra pseudorotunda can be distinguished, posterior to the apertura lateralis recessus scalae tympani (Fig. 3.1, 3.2). It opens in the juxstastapedial recess, just below the stapedial footplate, and represents the exit of the duct that originates in the foramen perilymphaticum (periotic foramen of Baird [1960]; primary perilymphatic foramen of McDowell [2008]) that opens into the

vestibulum (Baird, 1960). The fenestra pseudorotunda is notably larger than the apertura lateralis recessus scalae tympani as in uropeltoids (Fig. 3), whereas in *Anilius scytale* the two structures are equal in size (Rieppel, 1979a; pers. obs.). The right digital endocast of the inner ear (Fig. 4.2) exhibits the typical morphology shared by burrowing squamates including uropeltoid snakes (Olori, 2010; Yi, 2022), with a large globous vestibule as a most notable trait. Semicircular canals are wrapped tightly to the vestibule (Fig. 4.3) as in other burrowing snakes (Palci *et al*., 2017; Yi, 2022). The lateral semicircular canal is in contact with the vestibule in similar fashion to that seen in *Anilius scytale* and uropeltoids.

Anatomical analysis of cranial features related to burrowing and/or miniaturization

Surveyed burrowing and miniaturized surface-dwelling colubroideans have a very small body size, not surpassing 300 mm of snout-vent length; consequently, the skull of these species is also small, not exceeding 10 mm in snout-condyle length (Fig. 5.1. 5.2). Bones of the jaw apparatus exhibit a notable shortening and reduction of articular areas between them (Fig. 5.2), an allometric tendency that conforms a non-macrostomous skull (Scanferla, 2016). In general, we observe a marked shortening of the supratemporal in the selected cryptozoic colubroideans, not only the posterior free-ending process which is usually reduced in miniaturized snakes, but also the anterior part of this bone responsible to the attachment with the rest of the skull. In some species such as *Xenocalamus bicolor* and *Tantilla schistosa*, the anterior region of the supratemporal is greatly reduced, thus the anterior part of the cephalic condyle of the quadrate establishes contact with the prootic bone (Fig. 5.3) in similar fashion to that observed in some uropeltoid snakes such as *Anomochilus weberi* (Cundall & Rossman,

1993). In some small, colubroidean burrowing species such as *Calliophis gracilis* (Fig. 5.1), *Levitonius mirus* (Fig. 5.4) and *Calamaria pavimentata* the reduction of the supratemporal reaches an extreme and it remains as a small splint of bone attached to the internal region of the cephalic condyle of the quadrate, thus it cannot be observed in lateral view. There is a marked shortening of the quadrate bone in some species, such as *Calliophis gracilis* (Fig. 5.1) or *Geagras redimitus* where the quadrate is only two-thirds of the height of the neurocranium. Notably, the cephalic condyle of the quadrate of burrowing colubroideans remains proportionally large with respect to the rest of the bone and thus establishes a wide contact with the prootic (Fig. 5.3). However, the cephalic condyle of *Anomochilus* and uropeltid snakes is notably larger due to the posterior development of the suprastapedial process (Cundall & Irish, 2008; Olori & Bell, 2012).

Neurocranial bony elements remain unfused in most surveyed species of colubroideans, thus following the widespread condition in snakes (Fig. 5.1., 5.2, 5.5). Nevertheless, the basicranium (parabasisphenoid, basioccipital), prootics, otooccipitals and supraoccipital exhibit a complete fusion in *Xenocalamus bicolor* (Atractaspididae), *Geagras redimitus* (Colubridae), *Neelaps bimaculatus* (Elapidae) and *Levitonius mirus* (Cyclocoridae), thus conforming an occipital bone similar to that of uropeltids (Fig. 5.3, 5.4). Notably, other dermal neurocranial bones such as parietal and frontals remain as discrete bony elements in these snakes.

All species examined bear relatively large otic regions, evidenced by a large stapedial footplate closing the fenestra ovalis. Below the ventral rim of the fenestra ovalis, the apertura lateralis recessus scalae tympani can be seen; dorsally the recessus scalae tympani is perforated for the perilymphatic canal that communicates the vestibular chamber with the recessus scalae tympani. In contrast with this typical

arrangement of snake ear, burrowing and small surface-dwelling species such as the the dipsadid *Drepanoides anomalus*, the cyclocorid *Levitonius mirus* and the natricid *Aspidura brachyorrhos* exhibit another foramen above the apertura lateralis recessus scalae tympani (Fig. 5.4, 5.5). When the stapes is removed, it is clear that exists a short bony duct that communicates the vestibular chamber with the juxstastapedial chamber, in the same fashion that it is observed in *Anilius scytale* and uropeltoid snakes. Hence, we recognize this foramen as the fenestra pseudorotunda in these colubroideans. The dipsadid *Drepanoides anomalus* and the cyclocorid *Levitonius mirus* bear a large fenestra pseudorotunda and a small apertura lateralis recessus scalae tympani as in uropeltoid snakes (Fig. 3.3, 3.4, 3.5, 3.6), whereas these structures in *Aspidura brachyorrhos* are equal in size.

As in most extant snakes, all analyzed colubroideans consistently exhibit a fovea dentis in the dorsal region of the occipital condyle (Fig. 5.6, 6.1) including species with fused otooccipital and basioccipital bones. This configuration of the occipital condyle implies the lack of contact between the condylar processes of both otooccipitals, in contrast with the condition previously reported in *Anomochilus weberi* (Cundall & Rossman, 1993) but also noticeably in *Cylindrophis maculatus* (Fig. 6.3). In these uropeltoids, there is a contact of the condylary processes of the opposite otooccipital bones in the dorsal region of the occipital condyle and thus forming a very shallow fovea dentis (Fig 6.2, 6.3). In some small burrowing caenophidian species such as *Xenocalamus bicolor* and *Atractus poeppigi* (Fig. 6.1) the condylar process of the basioccipital is shorter than the condylar process of both otooccipitals, thus the occipital condyle acquires a saddle shape very similar to the condition present in some worm lizards such as *Leposternon* (Gans & Montero, 2008; pers. obs.).

Phylogenetic analysis

The maximum parsimony analysis resulted in four most parsimonious trees of 7800 steps each (CI = 0.40 - RI = 0.49). Our analysis included representatives of all snake clades, but we will focus our description of the phylogenetic results on the relationships within uropeltoids and other non-caenophidian alethinophidians. In the combined tree here (Fig. 7) *Anilius scytale* is the sister group of all other alethinophidians, in agreement with molecular and combined analyses that retrieved a polyphyletic "Anilioidea" (e.g. Scanlon & Lee, 2011; Pyron *et al*., 2013; Zheng & Wiens, 2016: Burbrink *et al.*, 2020). Notably, specimen MHAS 087 is deeply nested within a clade including species of *Cylindrophis*, *Anomochilus weberi* and the two sampled uropeltids *Melanophidium wynaudense* and *Rhinophis melanogaster* (Fig. 7). This clade is in congruence with recent phylogenies based on molecular and combined data (Gower *et al*., 2005; Pyron *et al.*, 2013; Zheng & Wiens, 2016: Burbrink *et al*., 2020) that retrieved a monophyletic Uropeltoidea. The most relevant morphological trait that supports this position is the anteroventral shift of the quadrate suspension with respect to the otic capsule due to the absence (or strong reduction) of the supratemporal (char. 175: 0 –›1). Moreover, MHAS 087 is recovered as a member of the family Uropeltidae because the spherical shape of the occipital condyle due to the absence of a fovea dentis (char. 177: 0 –›1) and the fusion of neurocranial bony elements (chars. 171: 0 –›1; 172: 0 –›1).

DISCUSSION

Anatomy

Since the phylogenetic studies based on molecular data (Heise *et al.*, 1995; Vidal & Hedges, 2002; Lee, 2005) and subsequent, best sampled phylogenies in terms of

terminal taxa and markers (Pyron *et al.*, 2013; Streicher & Wiens, 2017) the topology of the snake tree has greatly changed in comparison with morphology-based analyses. The paraphyly of blindsnakes ("Scolecophidia") and the paraphyletic nature of "anilioids" demonstrated that many morphological features previously thought to be diagnostic of these clades likely arose several times convergently along the history of snakes, correlated with miniaturization process characteristic of snakes that occupy underground habitats (Savitsky, 1983; Lee, 1998; Miralles *et al*., 2018; Strong *et al*., 2021a, 2021b). A partial or total fusion of neurocranial bones, enlarged inner ear and presence of a fenestra pseudorotunda in the inner ear constitute a combination of characters shared by specimen MHAS 087 and burrowing extant snakes.

Neurocranial bones of most alethinophidian snakes are largely unfused, thus being discrete elements throughout the postnatal ontogeny (Cundall & Irish, 2008). Exceptions of this general trend include the recently extinct *Bolyeria multocarinata* (Bolyeriidae) and uropeltids, which exhibit an extraordinary fusion of neurocranial bones similar to some blindsnakes (List, 1967; Rieppel, 1979b; Cundall & Irish, 2008; Olori & Bell, 2012). Notably, our survey of colubroideans revealed additional taxa with fusion of neurocranial bones among species that live underground, hence adding further support to this trend of morphological convergence.

As a distinct feature of the inner ear of snakes, the perilymphatic cistern of the membranous inner ear exits the inner ear cavity through the bony perilymphatic foramen and then projects outside creating the juxstastapedial sinus located in the lateral surface of the stapedial footplate (Baird, 1960; Miller, 1966, 1968). However, some snakes such as uropeltoids and *Anilius scytale* have a different arrangement of the membranous perilymphatic system, where the perilymphatic duct enters directly on the juxtastapedial recess through the fenestra pseudorotunda (Rieppel, 1979a; Rieppel &

385 Maisano, 2007). This fenestra was originally described by Rieppel (1979a) for
386 “anilioid” snakes (uropeltoids and *Anilius scytale*) and subsequently other authors
387 described the same feature in “anilioids” with different names (foramen pseudorotunda
388 and foramen rotunda of Cundall & Irish [2008]; foramen pseudorotundum of Olori &
389 Bell [2012]). The distribution of this different arrangement of the perilymphatic system
390 among burrowing snakes such as *Anilius scytale*, uropeltoids, and now in other snakes
391 such as specimen MHAS 087 and some surveyed colubroideans indicates a close
392 correlation between the presence of a fenestra pseudorotunda and burrowing habits.
393 However, the presence of this trait in the surface-dwelling colubroidean *Drepanoides*
394 *anomalus* suggest that this feature is not only correlated with burrowing. The complex
395 structure of the inner ear across the numerous clades of snakes certainly deserves further
396 analysis.
397 The spheric occipital condyle of MHAS 087 is noteworthy, being the only feature
398 that unambiguously provides evidence of uropeltid affinities for this fossil. The
399 spherical condyle of uropeltid snakes represents a special exception that contrasts with
400 the typical configuration of the occipital condyle in squamates, which is a kidney-
401 shaped structure in posterior view formed by the condylar process of both otooccipitals
402 laterally and the condylar process of the basioccipital ventrally. This unique
403 morphology of the uropeltid occipital condyle was previously reported by several
404 authors (Hoffstetter, 1939; Williams, 1958; Rieppel & Zaher, 2002; Cundall & Irish,
405 2008; Olori & Bell, 2012), which is part of the specialized cranio-vertebral joint and
406 possibly related to the “freight-train” burrowing locomotion of at least some uropeltids
407 (Gans *et al*., 1978). The fusion of neurocranial elements and lack of ontogenetic studies
408 of the uropeltid skull are impediments to know the anatomical transformations that
409 finally leads this spheric configuration. However, the “intermediate” morphology of the

occipital condyle in other uropeltoids such as *Cylindrophis maculatus* (Fig. 6.2) and *Anomochilus weberi* (Fig. 6.3) suggests that a midline contact between the condylar processes of the opposite otooccipital bones reduces drastically the size of the fovea dentis and thus emerges as a prerequisite to acquire a spherical condyle.

Phylogeny and paleobiogeography

Molecular and combined phylogenetic analyses, including this work, retrieve a monophyletic Uropeltoidea composed by uropeltids and species of the genera *Cylindrophis* and *Anomochilus* (e.g. Scanlon & Lee, 2011; Pyron *et al.*, 2013; Figueroa *et al*., 2016; Burbrink *et al*., 2020). Today, uropeltoid snakes are distributed mostly in forest and wetlands of peninsular India, Sri Lanka and Southeast Asia (Bossuyt *et al.*, 2004; Das *et al.*, 2008; Kieckbusch *et al.*, 2016, 2018). Based primarily on their current distribution, some authors have claimed that *Cylindrophis* and *Anomochilus* originated in the Indo-Malayan region (Bernstein *et al.*, 2020). The geographic distribution in Sri Lanka of *Cylindrophis maculatus*, the basalmost species of genus *Cylindrophis*, suggests that the origin of cylindrophiids occurred in the Indian subcontinent and then dispersed eastward to Southeast Asia.

Indian subcontinent moved north during the Late Cretaceous and Early Cenozoic, acting as a raft carrying the ancestors of several Southeast Asian clades from Gondwana to Eurasia on its northward journey, a paleobiogeographic scenario dubbed the ‘Out-of-India’ hypothesis. It has been invoked to explain the biogeographical history of many taxa, including plants, invertebrates and vertebrates (Bossuyt & Milinkovitch, 2001; Conti *et al*., 2002; Gower *et al*., 2002; Karanth, 2006; Data & Karanth, 2009; Svenson & Whiting, 2009; Klaus *et al*., 2010; Okajima & Kumazawa, 2010; Loria & Prendini, 2020). If the affinities between specimen MHAS 087 and

uropeltoid snakes are confirmed, the uropeltoid biogeography imply its origin in a Gondwanan terrain and a subsequent eastward interchange route to the rest of the Indo-Malayan region, rendering extant uropeltoids into Gondwanan relicts and thus supporting an Out-of-India scenario. Available temporally-calibrated trees and relaxed molecular clocks estimate the split between uropeltoids and the rest of alethinophidian snakes 90-64 million years ago (Vidal *et al.*, 2009; Cyriac & Kodandaramaiah, 2017; Klein *et al.*, 2021). Given that the onset of Gondwanan break-up happened mostly before this time interval, the potential presence of a uropeltoid in the Eocene of South America implies a transoceanic and/or island-hopping dispersion between West Gondwanan terrains (South America) and East Gondwanan terrains (India). This dispersal scenario seems to be plausible since there is a growing body of information that suggests a bidirectional faunistic and floristic interchange between these landmasses during the Campanian-Eocene time span (Ezcurra & Agnolin, 2012; Smith *et al.*, 2016; Prasad & Parmar, 2022).

Regrettably, there are no indisputable fossils attributed to uropeltoid snakes to directly test this probable Gondwanan origin of the group (Head, 2021; Head *et al.*, 2022; Smith & Georgalis, 2022). However, it is worth noting that many vertebrae recovered in Upper Cretaceous and Paleogene deposits of South America, Europe, Africa and India exhibit an "anilioid" grade morphology (Augé & Rage, 2006; Gómez et al., 2008; Rage *et al*., 2004, 2008, 2021). Although they can correspond with other burrowing snake clades even not yet recognized, it is not impossible that some of these vertebrae might correspond to uropeltoids.

Fragmentary fossils and their informativeness in times of "publish or perish"

Currently, the academic system exerts an increasing pressure upon scientists to reach a high publication output preferably in high-impact journals. This situation does not always promote positive outcomes, sometimes leading to unethical misconducts and ultimately undermine the scientific production in many different ways (Lawrence, 2007, 2016; Fanelli, 2012).

Relevant discoveries in the field such as transitional forms, new clades and/or paleobiogeographic puzzles undoubtedly push upward the publication scores of vertebrate paleontologists. These kinds of findings frequently derive in "positive narratives" of evolutionary trends, which are appealing narratives and constitute an important (un)conscious bias in evolutionary biology (Gould, 1992; Diogo, 2017). Although these kinds of discoveries are usually a by-product of hard fieldwork, they have an unavoidable chance component. Other more mundane ways to reach a bulky, high-rated research outcome are the atomization of results and sensationalism (the largest, the oldest). In snake paleontology, where fragmentary material largely constitute the norm (Rage, 1984) the inflation and over-interpretation of results is additionally complicated, sometimes leading to evolutionary scenarios based on isolated bone elements (e.g. Longrich *et al*., 2012; Fachini *et al*., 2021) that do not bring enough anatomical and/or phylogenetic information (Nydam *et al.*, 2014; Powers *et al.*, 2023). Regardless that the study of fragmentary snake specimens often constitutes the "only play in town" in ophidian paleontology (see Smith & Georgalis, 2022), and fragmentary specimens sometimes result a valuable source of information (Head et al., 2022; Smith & Georgalis, 2022) ultimately the researcher has the possibility to opt between a moderate best-supported report instead grandiloquent evolutionary scenarios barely underpinned by the evidence.

Despite our research counts with an exhaustive anatomical analysis and an explicit (cladistic) phylogenetic hypothesis, the fragmentary nature of specimen MHAS 087 prompts us to be cautious in our conclusions, especially considering the pervasive morphological convergence in the preserved skull traits among burrowing snakes. We believe a discreet analysis of fragmentary specimens contributes much better with a long research cycle about snake evolution to reduce the waste of resources in falsifying exaggerated or unsupported findings. Although the completeness of a specimen is not entirely correlated with its systematic informativeness, phylogenetic relationships improves when new and more complete specimens are found and its anatomical knowledge increases (Mannion & Upchurch, 2010, Driscoll *et al*., 2018; Schnetz *et al*., 2024). Thus, hard fieldwork ultimately will provide better fossils to confirm or refute the presence of uropeltoid snakes outside their current geographic distribution areas.

CONCLUSIONS

We report herein the presence of a burrowing small snake in Eocene levels of Geste Formation (Catamarca province, Argentina). With caveats concerning the incomplete nature of the analyzed specimen, the data and analyses presented here provide tentative evidence of a phylogenetic relationship between specimen MHAS 087 and Indomalayan uropeltoids. However, the pervasive morphological convergences that exists in the skeleton of burrowing and surface-dwelling miniaturized snakes suggests that some cranial features we recognize in this fossil could plausibly have been acquired independently (convergently) during the evolutionary history of ophidians and thus providing equivocal evidence about the phylogenetic relationships of this new specimen.

ACKNOWLEDGMENTS

The authors thank Gregory Schneider, Claudia Koch, Jennifer Olori, Filipa Sampaio, David Gower, Jessie Maisano and Matt Colbert to provide assistance during scanning and facilitated access to valuable CT data. As is indebted to Krister Smith who facilitated the scan of the specimen in Germany. We are also grateful to Nahuel Vega (Laboratorio Argentino de Haces de Neutrones, CNEA) for the access to CT facilities and technical support. This gratitude is extended to the staff of Digimorph, Morphosource and Phenome10K digital libraries. Fernando Garberoglio and David Gower made helpful suggestions that improved greatly this work. The phylogenetic analysis was performed with TNT, software that is freely available through the Willi Hennig Society. This work was funded by ANPCyT (PICT 2020-2443 to A.S.) and CONICET (PIP 0875 to A.S.). None of the contents of this manuscript (primary data, results, images) were created or analyzed with artificial intelligence.

REFERENCES

Albino, A. M. (2018). New macrostomatan snake from the Paleogene of northwestern Argentina. *Geobios, 51*, 175–179.

Augé, M., & Rage, J.-C. (2006). Herpetofaunas from the Upper Paleocene and Lower Eocene of Morocco. *Annales de Paleontologie, 92*, 235–253.

Babot, M. J., Aceñolaza, G., Carrizo, H. A. & García-López, D. A. (2018). Fossil record of the Puna. In H. Grau, M. J. Babot, A. Izquierdo & A. Grau (Eds.). *La Puna Argentina: Naturaleza y Cultura*. (pp. 117–140). Fundación Miguel Lillo.

Babot, M. J., Rougier, G. W., García-López D. A. & Davis, B. M. (2019). New small bunodont metatherian from the late Eocene of the Argentinean Puna. *Journal of Mammalian Evolution, 27*(3), 373–384.

533 Baird, I. L. (1960). A survey of the periotic labyrinth in some representative recent
534 reptiles. *University of Kansas Science Bulletin, 41*, 891–981.
535 Bernstein, J. M., Bauer, A. M., Mcguire, J. A., Arida, E., Kaiser, H., Kieckbusch, M., &
536 Mecke, S. (2020). Molecular phylogeny of Asian pipesnakes, genus *Cylindrophis*
537 Wagler, 1828 (Squamata: Cylindrophiidae), with the description of a new species
538 from Myanmar. *Zootaxa, 4851*, 535–558.
539 Bossuyt, F. & Milinkovitch, M. C. (2001). Amphibians as indicators of Early Tertiary
540 "Out-of-India" dispersal of vertebrates. *Science, 292*, 93–95.
541 Bossuyt, F., Meegaskumbura, M., Beenaerts, N., Gower, D. J., Pethiyagoda, R.,
542 Roelants, K., Mannaert, A., Wilkinson, M., Bahir, M. M., Manamendra-Arachchi,
543 K., Ng, P. K. L., Schneider, C. J., Oommen, O. V., & Milinkovitch, M. C. (2004).
544 Local endemism within the western Ghats-Sri Lanka biodiversity hotspot.
545 *Science, 306*, 479–481.
546 Burbrink, F. T., Grazziotin, F. G., Pyron, R. A., Cundall, D., Donnellan, S., Irish, F.,
547 Keogh, J. S., Kraus, F., Murphy, R. W., Noonan, B., Raxworthy, C. J., Ruane, S.,
548 Lemmon, A. R., Lemmon, E. M., & Zaher, H. (2020). Interrogating Genomic-
549 Scale Data for Squamata (Lizards, Snakes, and Amphisbaenians) Shows no
550 Support for Key Traditional Morphological Relationships. *Systematic Biology,*
551 *69*(3), 502–520.
552 Ciancio, M. R., Herrera, C., Aramayo, A., Payrola Bosio, P. & Babot, M. J. (2016).
553 Diversity of cingulate xenarthrans in the middle-late Eocene of northwestern
554 Argentina. *Acta Palaeontologica Polonica, 61*, 575–590.
555 Conti, E., Eriksson, T., Schönenberger, J., Sytsma, K. J. & Baum, D. A. (2002). Early
556 Tertiary Out-of-India dispersal of Crypteroniaceae: Evidence from phylogeny and
557 molecular dating. Evolution 56, 1931–1942.

558 Cundall, D. & Rossman, D. A. (1993). Cephalic anatomy of the rare Indonesian snake
559 *Anomochilus weberi*. *Zoological Journal of the Linnean Society, 109*, 235-273.
560 Cundall, D., & Irish, F. J. (2008). The snake skull. In C. Gans, A. S. Gaunt & K. Adler
561 (Eds.). *Biology of the Reptilia, volume 20, Morphology H. The skull of*
562 *Lepidosauria* (pp. 349–692). Society for the Study of Amphibians and Reptiles.
563 Cyriac, V. P., & Kodandaramaiah, U. (2017). Paleoclimate determines diversification
564 patterns in the fossorial snake family Uropeltidae Cuvier, 1829. *Molecular*
565 *Phylogenetics and Evolution, 116*, 97–107.
566 Das, I., Lakim, M., Lim, K. K. P., & Hui, T. H. (2008). New Species of *Anomochilus*
567 from Borneo (Squamata: Anomochilidae). *Journal of Herpetology, 42*, 584–591.
568 Datta-Roy, A. & Karanth, K. P. (2009). The Out-of-India hypothesis: What do
569 molecules suggest? *Journal of Biosciences, 34*, 687–697.
570 DeCelles, P. G., Carrapa, B. & Gehrels, G. E. (2007). Detrital zircon U-Pb ages provide
571 provenance and chronostratigraphic information from Eocene synorogenic
572 deposits in northwestern Argentina. *Geology, 35*, 323–326.
573 Diogo, R. (2017). *Evolution driven by organismal behavior: a unifying view of life,*
574 *function, form, mismatches, and trends*. Springer.
575 Driscoll, D. A., Dunhill, A. M., Stubbs, T. L., & Benton, M. J. (2018). The Mosasaur
576 fossil record through the lens of fossil completeness. *Palaeontology, 62*, 51–75.
577 Ezcurra, M. D., & Agnolín, F. L. (2012). A new global palaeobiogeographical model
578 for the late Mesozoic and early Tertiary. *Systematic Biology, 61*, 553–66.
579 Fachini, T, Onary, S., Palci, A, Lee, M. S. Y., Bronzati, M. & Hsiou, A. (2021).
580 Cretaceous blind snake from Brazil fills major gap in snake evolution. *iScience,*
581 *24*, 102180.

582 Fanelli, D. (2012). Negative results are disappearing from most disciplines and
583 countries. *Scientometrics, 90*, 891–904.
584 Farris, J. S. (1983). The logical basis of phylogenetic analysis. In N. I. Platnick & V. A.
585 Funk (Eds.), *Advances in cladistics, vol. II* (pp. 7–36). Columbia University Press.
586 Figueroa, A., McKelvy, A. D., Grismer, L. L., Bell, C. D. & Lailvaux, S. P. (2016). A
587 species-level phylogeny of extant snakes with description of a new colubrid
588 subfamily and genus. *PLoS ONE, 11*(9), e0161070.
589 https://dx.doi.org/10.1371/journal.pone.0161070
590 Forstner, M. R. J., Davis, S. K., & Arévalo, E. (1995). Support for the hypothesis of
591 anguimorph ancestry for the suborder Serpentes from phylogenetic analysis of
592 mitochondrial DNA sequences. *Molecular Phylogenetics and Evolution, 4*, 93–
593 102.
594 Gans, C. & Montero, R. (2008). An atlas of amphisbaenian skull anatomy. In C. Gans,
595 A. S. Gaunt & K. Adler (Eds.). *Biology of the Reptilia, volume 20, Morphology H.*
596 *The skull of Lepidosauria* (pp. 621–738). Society for the Study of Amphibians
597 and Reptiles.
598 Gans, C., Dessauer, H.C. & Baic, D. (1978). Axial differences in the musculature of
599 uropeltid snakes: The freight-train approach to burrowing. *Science, 199*, 189–192.
600 Garberoglio, F. F., Triviño, L. N. & Albino, A. (2022). A new madtsoiid snake from the
601 Paleogene of South America (northwestern Argentina), based on an articulated
602 postcranial skeleton. Journal of Vertebrate Paleontology, 42, e2128687.
603 https://doi.org/10.1080/02724634.2022.2128687
604 García-López, D. A. & Babot, M. J. (2015). Notoungulate faunas of northwestern
605 Argentina: recent findings on Eocene early diverging forms. *Journal of Systematic*
606 *Palaeontology*, *13*, 557–579.

607 Goloboff, P. A. & Morales, M. E. (2023). TNT version 1.6, with a graphical interface
608 for MacOS and Linux, including new routines in parallel. *Cladistics*, *39*, 144–153.
609 Gómez, R. O., Baez, A. M. & Rougier, G. W. (2008). An anilioid snake from the Upper
610 Cretaceous of northern Patagonia. *Cretaceous Research*, *29*, 481–488.
611 Gómez, R. O., Turazzini, G. F., García-López, D. A. & Babot, M. J. (2025). A late
612 Eocene frog assemblage from the Geste Formation, Puna of north-western
613 Argentina. *Historical Biology*, *37*(3), 621–642.
614 Gould, S. J. (2002). *The structure of evolutionary theory*. Harvard University Press.
615 Gower, D. J., Kupfer, A., Oommen, O. V., Himstedt, W., Nussbaum, R. A., Loader, S.
616 P., Presswell, B., Muller, E., Krishna, S. B., Boistel, R. & Wilkinson, M. (2002).
617 A molecular phylogeny of ichthyophiid caecilians (Amphibia: Gymnophiona:
618 Ichthyophiidae): Out of India or out of South East Asia? *Proceedings of the Royal*
619 *Society of London B*, *269*, 1563–1569.
620 Gower, D. J., Vidal, N., Spinks, J. N., & McCarthy, C. J. (2005). The phylogenetic
621 position of Anomochilidae (Reptilia: Serpentes): first evidence from DNA
622 sequences. *Journal of Zoological Systematics and Evolutionary Research*, *43*,
623 315–320.
624 Hall, T. A. (1999). BioEdit: a user-friendly biological sequence alignment editor and
625 analysis program for Windows 95/98/NT. *Nucleic Acids Symposium Series*, *41*,
626 95–98.
627 Head, J. J. (2021). A South American snake lineage from the Eocene Greenhouse of
628 North America and a reappraisal of the fossil record of “anilioid” snakes.
629 *Geobios*, *66-67*, 55–65.
630 Head, J. J., Howard, A. F. C., & Müller, J. (2022). The First 80 Million Years of Snake
631 Evolution: The Mesozoic Fossil Record of Snakes and Its Implications for Origin

Hypotheses, Biogeography, and Mass Extinction. In D. J. Gower & H. Zaher (Eds.). *The Origin and Early Evolutionary History of Snakes* (pp. 26–54). Cambridge University Press.

Heise, P. J., Maxson, L. R., Dowling, H. G., & Hedges, S. B. (1995). Higher-level snake phylogeny inferred from mitochondrial DNA sequences of 12S rRNA and 16S rRNA genes. *Molecular Biology and Evolution*, *12*, 259–265.

Hoffstetter, R. (1939). Sur l'articulation occipito-vertebrale des Uropeltidae (ophidiens fouisseurs). *Bulletin du Muséum d'Histoire Naturelle Paris, 11*, 426–433.

Karanth, K. P. (2006). Out-of-India Gondwana origin of some tropical Asian biota. *Current Science, 90*, 789–792.

Klaus, S., Schubart, C. D., Streit, B. & Pfenninger, M. (2010). When Indian crabs were not yet Asian—biogeographic evidence for Eocene proximity of India and Southeast Asia. *BMC Evolutionary Biology, 10*, 287. https://doi.org/10.1186/1471-2148-10-287.

Kieckbusch, M., Mader, F., Kaiser, H., & Mecke, S. (2018). A new species of *Cylindrophis* Wagler, 1828 (Reptilia: Squamata: Cylindrophiidae) from Boano Island, northern Maluku Province, Indonesia. *Zootaxa, 4486 (3)*, 236–250.

Kieckbusch, M., Mecke, S., Hartmann, L., Ehrmantraut, L., O'Shea, M., & Kaiser, H. (2016). An inconspicuous, conspicuous new species of Asian pipesnake, genus *Cylindrophis* (Reptilia: Squamata: Cylindrophiidae), from the south coast of Jawa Tengah, Java, Indonesia, and an overview of the tangled taxonomic history of *C. ruffus* (Laurenti, 1768). *Zootaxa, 4093*(1), 1–25.

Klein, C. G., Pisani, D., Field, D. J., Lakin, R., Wills, M. A., & Longrich, N. R. (2021). Evolution and dispersal of snakes across the Cretaceous-Paleogene mass

656 extinction. *Nature Communications, 12*, 5335. https://doi.org/10.1038/s41467-
657 021-25136-y
658 Lawrence, P. A. (2007). The mismeasurement of science. Current Biology, 17, R583-5.
659 https://doi.org/10.1016/j.cub.2007.06.014.
660 Lawrence, P. A. (2016). The Last 50 Years: Mismeasurement and Mismanagement Are
661 Impeding Scientific Research. *Current Topics in Developmental Biology, 20*,
662 617–631. https://doi.org/10.1016/bs.ctdb.2015.12.013
663 Ledesma, J., del Papa, C. & Payrola, P. (2019). Revisión de la estratigrafía eocena-
664 pliocena de la cuenca intermontana de San Antonio de los Cobres, puna salteña,
665 Argentina. *Latin American Journal of Sedimentology and Basin Analysis, 26*, 57–
666 73.
667 Lee, M. S. Y. (1998). Convergent evolution and character correlation in burrowing
668 reptiles: towards a resolution of squamate relationships. *Biological Journal of the*
669 *Linnean Society, 65*, 369–453.
670 Lee, M. S. Y. (2005). Molecular evidence and snake origins. *Biology Letters, 1*, 227–
671 230.
672 List, J. C. (1966). Comparative osteology of the snake families Typhlopidae and
673 Leptotyphlopidae. *Illinois Biological Monographs, 36*, 1–112.
674 Longrich, N. R., Bhullar, B-A. S., & Gauthier, J. A. (2012). A transitional snake from
675 the Late Cretaceous period of North America. *Nature, 488*, 205–208.
676 López, G. M. (1997). Paleogene faunal assemblage from Antofagasta de la Sierra
677 (Catamarca Province, Argentina). *Paleovertebrata, 26*, 61–81.
678 Loria, S. F., & Prendini, L. (2020). Out of India, thrice: diversification of Asian forest
679 scorpions reveals three colonizations of Southeast Asia. *Scientific Reports, 10*,
680 22301. https://doi.org/10.1038/s41598-020-78183-8.

Maddison, W. P., & Maddison, D. R. (2007). Mesquite: a modular system for evolutionary analysis. Version 2.0., from http://mesquiteproject.org

Mannion, P. D., & Upchurch, P. (2010). Completeness metrics and the quality of the sauropodomorph fossil record through geological and historical time. *Paleobiology, 36*, 283–302.

McDowell, S. B. (2008). The Skull of Serpentes. In C. Gans, A. S. Gaunt & K. Adler (Eds.). *Biology of the Reptilia, volume 24, Morphology H. The skull and appendicular locomotor apparatus of Lepidosauria* (pp 467–620). Society for the Study of Amphibians and Reptiles.

Miller, M. R. (1966). The cochlear duct of lizards and snakes. *American Zoologist, 6*, 421–429.

Miller, M. R. (1968). The cochlear duct of snakes. *Proceedings of the California Academy of Sciences, 35*, 425–476.

Miralles, A., Marin, J., Markus, D., Herrel, A., Hedges, S. B., & Vidal, N. (2018). Molecular evidence for the paraphyly of Scolecophidia and its evolutionary implications. *Journal of Evolutionary Biology, 31*, 1782–1793.

Nydam, R., Caldwell, M., &Palci, A. (2014). Reassessment of cranial elements assigned to the fossil snake *Coniophis precedens*, Late Cretaceous, North America. 74th SVP Annual Meeting (pp. 196–197). Berlin.

Okajima, Y., & Kumazawa, Y. (2010). Mitochondrial genomes of acrodont lizards: Timing of gene rearrangements and phylogenetic and biogeographic implications. *BMC Evolutionary Biology, 10*, 141. https://doi.org/10.1186/1471-2148-10-141.

703 Olori, J. C. (2010). Digital endocasts of the cranial cavity and osseous labyrinth of the
704 burrowing snake *Uropeltis woodmasoni* (Alethinophidia: Uropeltidae). *Copeia, 2010,* 14–26.
706 Olori, J. C., & Bell, C. J. (2012). Comparative skull morphology of uropeltid snakes
707 (Alethinophidia: Uropeltidae) with special reference to disarticulated elements
708 and variation. *PLoS ONE, 7(3),* e32450.
709 https://doi.org/10.1371/journal.pone.0032450
710 Palci, A., Hutchinson, M. N., Caldwell, M. W., & Lee, M. S. Y. (2017). The
711 morphology of the inner ear of squamate reptiles and its bearing on the origin of
712 snakes. *Royal Society Open Science, 4*, 170685.
713 Powers, M. J., Nydam, R., & Caldwell, M. W. (2023). The lion, the goat, the snake and
714 a hero: defeating chimeras using the "Bellerophon method". 83rd SVP Annual
715 Meeting (pp. 351–352). Cincinnati.
716 Prasad, G. V. R. & Parmar, V. (2022). Cretaceous insular India – Consequences for
717 biological evolution and faunal interchanges. *Journal of the Palaeontological*
718 *Society of India, 67(1),* 56–71.
719 Pyron, R. A., Burbrink, F. T., & Wiens, J. J. (2013). A phylogeny and revised
720 classification of Squamata, including 4161 species of lizards and snakes. *BMC*
721 *Evolutionary Biology, 13(93)*. http://doi.org/10.1186/1471-2148-13-93
722 Rage., J.-C. (1974). Les serpents des phosphorites du Quercy. *Palaeovertebrata, 6,*
723 274–303.
724 Rage, J.-C. (1984). Handbuch der Paläoherpetologie. Teil 11, Serpentes. Gustav Fischer
725 Verlag, Stuttgart.
726 Rage, J-C., Adaci, M., Bensala, M., Mahboubi, M., Marivaux, L., Mebrouk, F., &
727 Tabuce, R. (2021). Latest Early-early Middle Eocene deposits of Algeria (Glib

728 Zegdou, HGL50), yield the richest and most diverse fauna of amphibians and
729 squamate reptiles from the Palaeogene of Africa. *Palaeovertebrata*, *44*(1), e1.
730 http://doi.org/10.18563/pv.44.1.e1
731 Rage, J.−C., Folie, A., Rana, R. S., Singh, H., Rose, K. D., & Smith, T. (2008). A
732 diverse snake fauna from the early Eocene of Vastan Lignite Mine, Gujarat, India.
733 *Acta Palaeontologica Polonica, 53*(3), 391–403.
734 Rage, J. C., Prasad, G. V. R., & Bajpai, S. (2004). Additional snakes from the
735 uppermost Cretaceous (Maastrichtian) of India. *Cretaceous Research, 25*, 425–
736 434.
737 Reguero, M. A., Croft, D. C., López, G. & Alonso, R. N. (2008). Eocene
738 archaeohyracids (Mammalia: Notoungulata: Hegetotheria) from the Puna,
739 northwest Argentina. *Journal of South American Earth Sciences, 26*, 225–233.
740 Rieppel, O. (1979a). The evolution of the basicranium in the Henophidia (Reptilia:
741 Serpentes). *Zoological Journal of Linnean Society, 66*, 411–431.
742 Rieppel, O. (1979b). The braincase of *Typhlops* and *Leptotyphlops* (Reptilia: Serpentes).
743 *Zoological Journal of Linnean Society, 65*, 161–176.
744 Rieppel, O., & Zaher, H. (2002). The skull of the Uropeltinae (Reptilia, Serpentes), with
745 special reference to the otico-occipital region. *Bulletin Natural History Museum*
746 *London (Zoology), 68*, 123–130.
747 Rieppel, O. & Maisano, J. A. (2007). The skull of the rare Malaysian snake
748 *Anomochilus Leonardi* Smith, based on high-resolution X-ray computed
749 tomography. *Zoological Journal of the Linnean Society, 149*, 671–685.
750 Savitsky, A. H. (1983). Coadapted character complexes among snakes: fossoriality,
751 piscivory, and durophagy. *American Zoologist, 23*, 397–409.
752 Scanferla, A. (2016). Postnatal ontogeny and the evolution of macrostomy in snakes.

Royal Society Open Science, 3, 160612. http://dx.doi.org/10.1098/rsos.160612

Scanferla, A. Smith, K. T., & Schaal, S. F. K. (2016). Revision of the cranial anatomy and phylogenetic relationships of the Eocene minute boas *Messelophis variatus* and *Messelophis ermannorum* (Serpentes, Booidea). *Zoological Journal of Linnean Society, 176*, 182–206.

Scanlon, J. D. & Lee, M. S. Y. (2011). The major clades of living snakes: Morphological evolution, molecular phylogeny, and divergence dates. In R. D. Aldridge & D. M. Sever (Eds.). *Reproductive biology and phylogeny of snakes* (pp. 55–95). CRC Press.

Schnetz, L., Butler, R. J., Coates, M. I., & Sansom, I. J. (2024). The skeletal completeness of the Palaeozoic chondrichthyan fossil record. *Royal Society Open Science, 11*, 231451. https://doi.org/10.1098/rsos.231451

Smith, K. T., & Georgalis, G. L. (2022). *The Diversity and Distribution of Palaeogene Snakes: A Review with Comments on Vertebral Sufficiency.* In D. J. Gower & H. Zaher (Eds.). *The Origin and Early Evolutionary History of Snakes* (pp. 55–84). Cambridge University Press.

Smith, T., Kumar, K., Rana, R. S., Folie, A., Solé, F., Noiret, C., Steeman, T., Sahni, A. & Rose, K. D. (2016). New early Eocene vertebrate assemblage from western India reveals a mixed fauna of European and Gondwana affinities. *Geoscience Frontiers, 7*, 969–1001.

Streicher, J. W., & Wiens, J. J. (2017). Phylogenomic analyses of more than 4000 nuclear loci resolve the origin of snakes among lizard families. *Biology Letters, 13*, 20170393. https://doi.org/10.1098/rsbl.2017.0393

776 Strong, C. R. C., Palci, A., & Caldwell, M. W. (2021a). Insights into skull evolution in
777 fossorial snakes, as revealed by the cranial morphology of *Atractaspis irregularis*
778 (Serpentes: Colubroidea). *Journal of Anatomy, 238,* 146–172.
779 Strong, C. R. C., Scherz, M. D. & Caldwell, M. W. (2021b). Deconstructing the Gestalt:
780 New concepts and tests of homology, as exemplified by a re-conceptualization of
781 "microstomy" in squamates. *Anatomical Record, 304,* 2303–2351.
782 Svenson, G. J. & Whiting, M. F. (2009). Reconstructing the origins of praying mantises
783 (Dictyoptera, Mantodea): The roles of Gondwanan vicariance and morphological
784 convergence. *Cladistics, 25*, 468–514.
785 Thompson, J. D., Gibson, T. J., Plewniak, F., & Jeanmougin, F. (1997). The Clustal
786 windows interface: flexible strategies for multiple sequence alignment aided by
787 quality analysis tools. *Nucleic Acids Research, 25,* 4876–4882.
788 Vidal, N., & Hedges, S. B. (2002). Higher-level relationships of snakes inferred from
789 four nuclear and mitochondrial genes. *Comptes Rendus Biologie, 325*, 977–985.
790 Vidal, N., & Hedges, S. B. (2005). The phylogeny of squamate reptiles (lizards, snakes,
791 and amphisbaenians) inferred from nine nuclear protein-coding genes. *Comptes*
792 *Rendus Biologies, 328*, 1000–1008
793 Vidal, N., Rage, J-C., Couloux, A., & Hedges, S. B. (2009). Snakes (Serpentes). In S.
794 B. Hedges & K. Kumar (Eds.). *The Timetree of Life* (pp. 390–397). Oxford
795 University Press.
796 Williams, E. E. (1959). The occipito–vertebral joint in the burrowing snakes of the
797 family Uropeltidae. *Breviora, 106*, 1–10.
798 Yi, H. (2022). Using adaptive traits in the ear to estimate ecology of early snakes. In D.
799 Gower & H. Zaher (Eds.). *The Origin and Early Evolution of Snakes* (pp. 271–
800 293). Cambridge University press.

801 Zheng, Y., & Wiens, J. J. (2016). Combining phylogenomic and supermatrix
802 approaches, and a time-calibrated phylogeny for squamate reptiles (lizards and
803 snakes) based on 52 genes and 4162 species. *Molecular Phylogenetics and*
804 *Evolution, 94*, 537–547.
805

Appendix. **Specimens examined**

MorphoSource specimens. *Diadophis punctatus* UMMZ herp 112146, *Contia tenuis* UMMZ herp 214408, *Gomesophis brasiliensis* UMMZ herp 218587, *Sonora semiannulata* CAS herp 206503, *Ficimia streckeri* UMMZ herp 101218, *Levitonius mirus* KUH 337269, *Xenocalamus bicolor* CAS Herp 248601, *Aparallactus modestus* CAS herp 111865, *Brachyorrhos albus* MCZ R 177248, *Apostolepis assimilis* UMMZ 204112, *Homoroselaps lacteus* CAS Herp 173258, *Scolecophis atrocinctus* UMMZ herp 131471, *Calamaria pavimentata* UMMZ herp 190533, *Chilorhinophis geradi* CAS herp 159106, *Elapomorphus mertensi* UMMZ Herp 63022, *Sinomicrurus annularis* MCZ 43047, *Tantilla schistosa* UMMZ herp 155726, *Atractus poeppigi* INPA 18518, *Apostolepis assimilis* UMMZ herp 204112, *Geophis hoffmani* UMMZ herp 238749, *Paikwaophis kruki* RBINS 2734, *Drepanoides anomalus* UMMZ herp 246795, *Calliophis gracilis* FMNH 178400, *Micrurus fulvius* UMMZ herp 128569, *Vermicella annulata* UMMZ herp 65820, *Aspidura brachyorrhos* CAS Herp 17206, *Achalinus spinalis* KUH 312259, *Neelaps bimaculatus* CUMV R-12301. *Melanophidium wynaudense* CAS herp 39633, *Platyplectrurus madurensis* CAS herp 244431, *Teretrurus sanguineus* CAS herp 226618, *Uropeltis woodmasoni* CG 1694 , *Rhinophis sanguineus* UF H 78397, *Plectrurus perrotteti* FMNH H 171566, *Cylindrophis maculatus* MCZ R 48944, *Cylindrophis ruffus* UMMZ 201901, *Cylindrophis aruensis* FMNH 60958, *Anomochilus leonardi* RIM 0026, *Anomochilus weberi* RMNH RENA 4691, *Anilius scytale* UMMZ 68003.

Dry Skeletons. *Achalinus formosanus* (LSUMZ 19354; BMNH 1983-192; *Anilius scytale* (CENAI 3883, MACN 8817a, MACN 8817b, IB 46686, MZ 14572); *Antaresia childreni*

(AMNH 86213); *Apostolepis erythronota* (AMNH 62192); *Apostolepis flavotorquata* (AMNH 93559); *Aspidites melanocephala* (AMNH 18681); *Atractaspis irregularis* (MNHN 1991.4071/4072); *Cylindrophis maculatus* (AMNH 85496); *Cylindrophis ruffus* (AMNH 85647, CM 147774, MNHN 1970.411); *Homoroselaps lacteus* (MNHN 1991.4162); *Hydrophis* sp. (MNHN 1986.0596); *Loxocemus bicolor* (AMNH 110151, MZUSP 14114, FML 970, LSUMZ 49634); *Oxyrhabdium modestum* (LSUMZ 11814); *Pseudotyphlops philippinus* (BMNH 1978.1092); *Uropeltis brevis* (BMNH); *Uropeltis ceylonicus* (AMNH 43343); *Uropeltis pulmeyensis* (MNHN 1994-756); *Xenopeltis unicolor* (MACN 7568, MZUSP 9665, MNHN 1991.4446, FMNH 11524); *Xylophis perroteti* (MNHN 1991.4426).

842 **Figure 1. 1**, Geographic location of the Geste Formation outcrops that yielded the
843 specimen **MHAS** 087, Antofagasta de la Sierra (Catamarca, Argentina). **2,** specimen
844 **MHAS** 087 in a silhouette of the skull of the uropeltoid snake ***Teretrurus sanguineus***
845 (**CAS** 244362). Scale bar equals 5 mm.
846
847 **Figure 2.** Specimen **MHAS** 087 in **1,** right lateral; **2,** left lateral; **3,** anterior; **4,**
848 posterior; **5,** dorsal; and **6,** ventral views. Dashed lines indicate eroded/missing parts.
849 Scale bar equals to 6 mm.
850
851 **Figure 3.** Posteroventral view of left (1) and right (2) ear region of specimen **MHAS**
852 087. Left lateral view of the neurocranium of ***Melanophidium wynaudense*** (**CAS**
853 39633) (3), ***Teretrurus sanguineus*** (**CAS** 226618) (4) ***Cylindrophis maculatus*** (**MCZ**
854 **R** 48944) (5) and ***Anomochilus weberi*** (**RMNH RENA** 4691) (6). Quadrate bone,
855 supratemporal and stapes were removed. Dotted line denotes the contact surface with
856 the quadrate bone. Dashed lines indicate digitally removed parts of the crista
857 circumfenestralis. Black arrow shows the passage of the perilymphatic duct. Scale bars
858 equal 2 mm.
859
860 **Figure 4. 1,** right and left stapes of specimen **MHAS** 087 in lateral view; **2,** digital
861 endocast of right inner ear of specimen **MHAS** 087 in lateral and medial views; **3,**
862 lateral and medial view of the digital endocast of right inner ear of the uropeltoid
863 ***Cylindrophis aruensis*** (**FMNH** 60958). Dashed lines indicate missing parts of the
864 semicircular canals. Scale bars equal 2 mm.
865
866 **Figure 5.** Skull anatomy of miniaturized cryptozoic and surface-dwelling

colubroideans. **1,** left lateral view of the skull and lower jaw of the elapid ***Calliophis gracilis*** (**CAS** 178400); **2,** ventral view of the skull of the atractaspidid ***Homoroselaps lacteus*** (**CAS** 173258); **3,** left anterolateral view of the neurocranium of the atractaspidid ***Xenocalamus bicolor*** (**CAS** 248601); **4,** Lateral view of the neurocranium of the cyclocorid ***Levitonius mirus*** (**KU** 337269); **5,** lateral view of the neurocranium of the dipsadid ***Drepanoides anomalus*** (**UMMZ** 246795); **6,** posterior view of the neurocranium of ***Homoroselaps lacteus*** (**CAS** 173258). Elements of the jaw apparatus were removed, dashed lines indicate removed parts of the crista circumfenestralis, and black arrows show the passage of the perilymphatic duct. Scale bars equal 2 mm.

Figure 6. 1, Posterior view of the skull of the dipsadid ***Atractus poeppigi*** (**INPA** 18518); **2,** the uropeltoid ***Anomochilus weberi*** (**RMNH RENA** 4691); **3,** the uropeltoid ***Cylindrophis maculatus*** (**MCZ R** 48944); and **4,** the uropeltid ***Teretrurus sanguineus*** (**CAS** 226618). Scale bars equal 2 mm.

Figure 7. Simplified strict consensus cladogram of the four most parsimonious trees obtained (tree length, L = 7800) based on the combined analysis of morphological, mitochondrial, and nuclear data partitions. snake relationships depicting the placement of specimen **MHAS** 087.

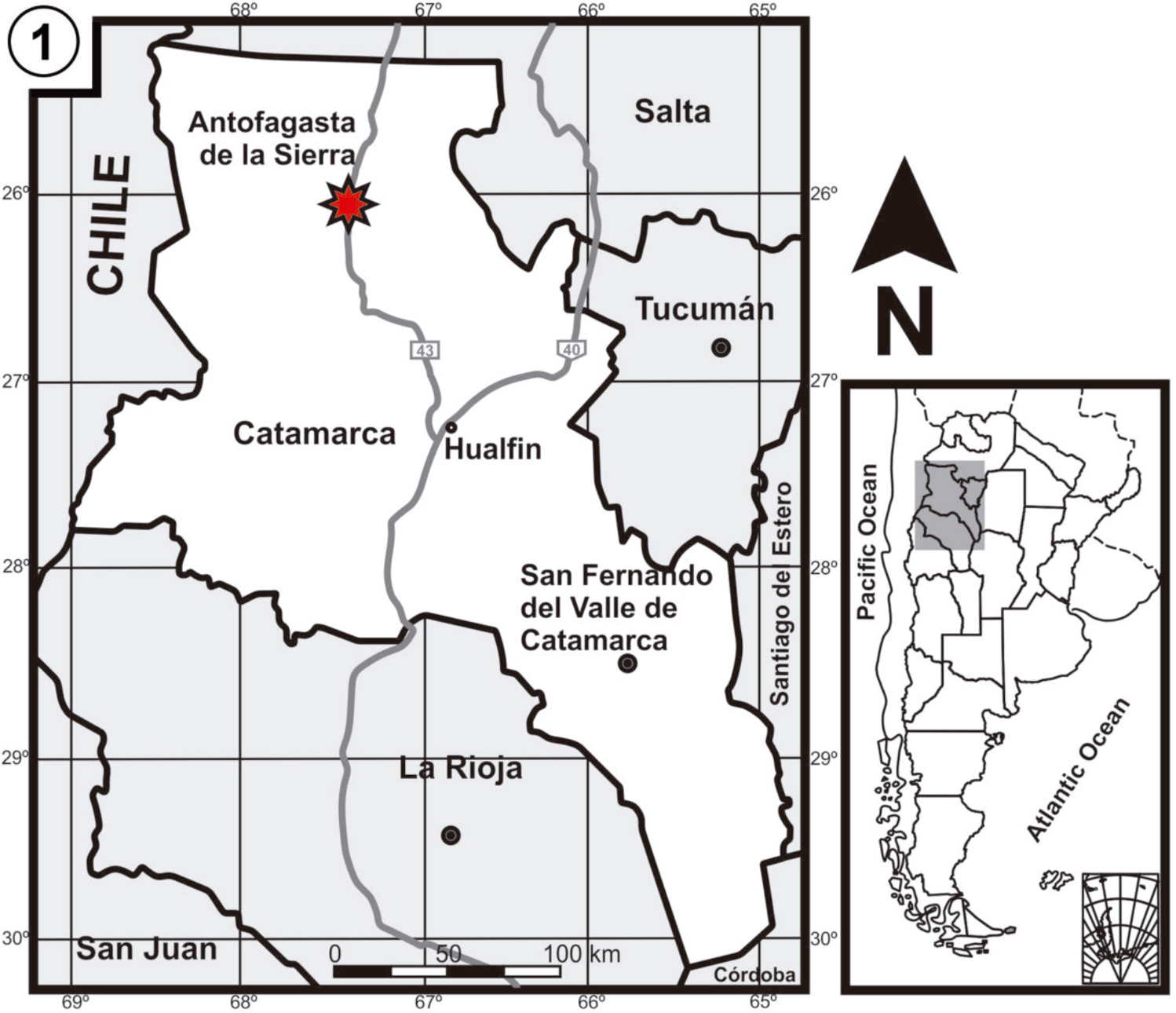
1
68°
67°
66°
65°
Antofagasta
de la Sierra
Salta
CHILE
26°
Tucumán
N
43
40
27°
Catamarca
Hualfin
Pacific Ocean
Santiago del Estero
San Fernando
del Valle de
Catamarca
28°
Atlantic Ocean
29°
La Rioja
30°
San Juan
0
50
100 km
Córdoba
69°

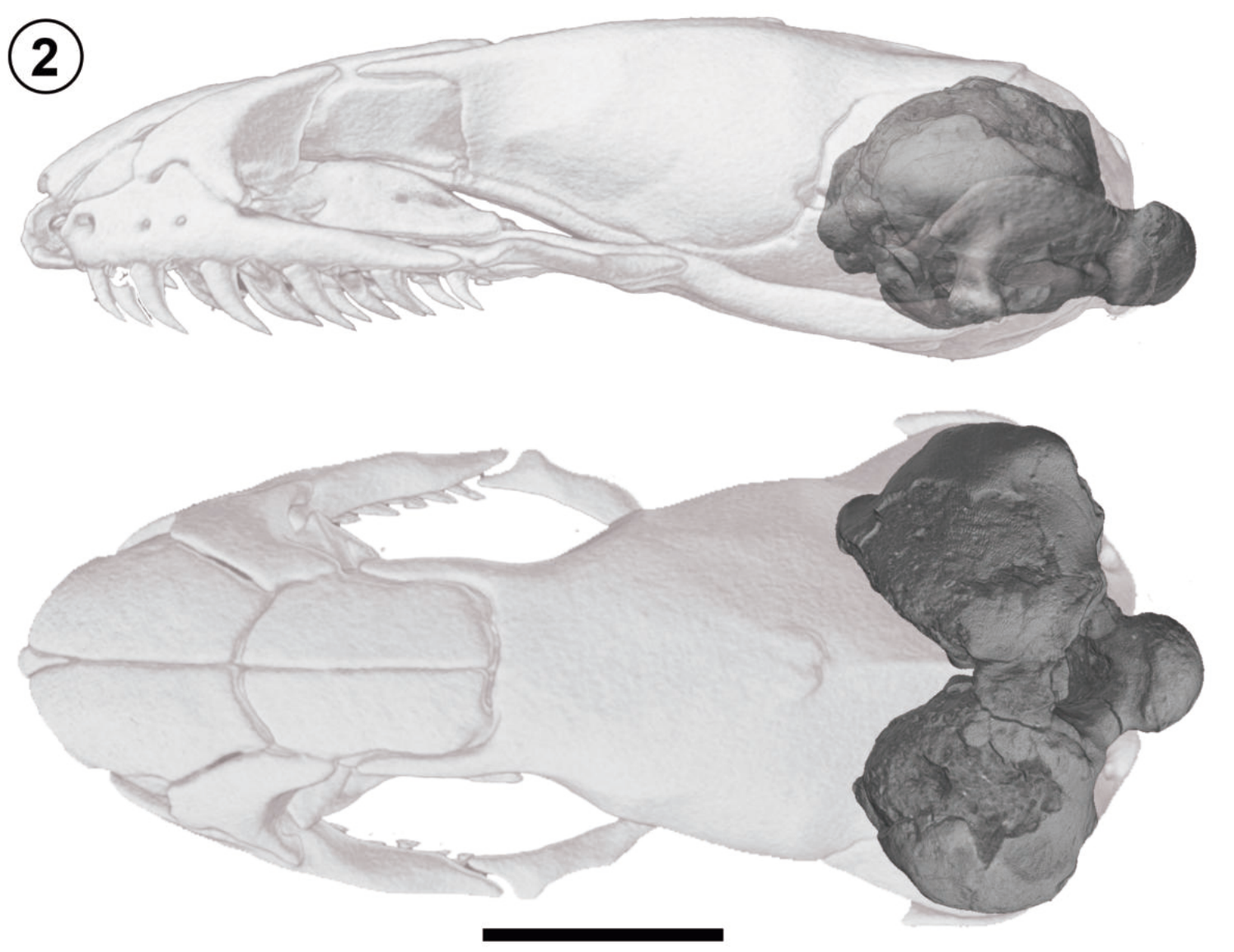
2

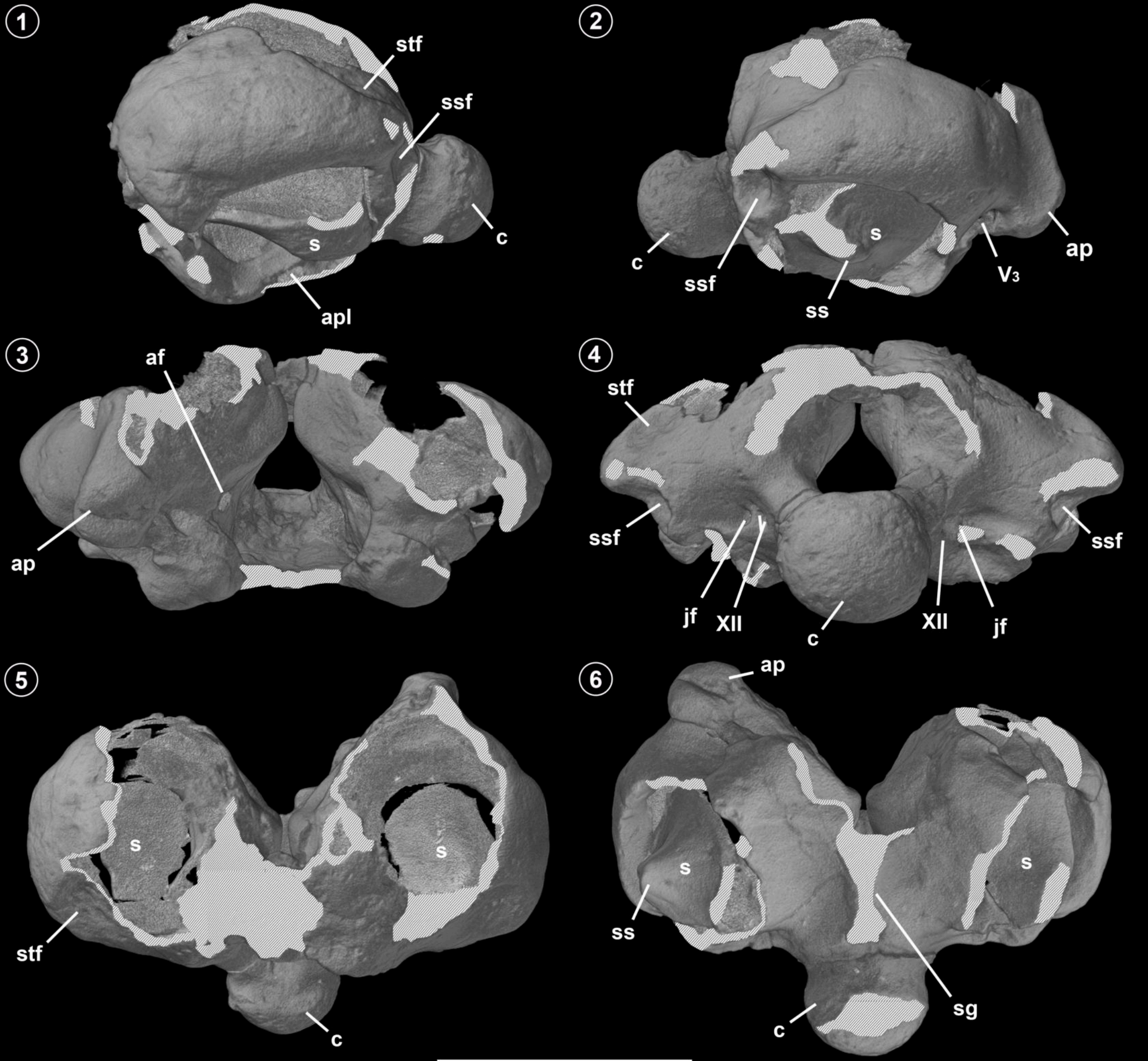
1
stf
ssf
c
s
apl
2
c
ssf
s
ss
V3
ap
3
af
ap
4
stf
ssf
jf
XII
c
XII
jf
ssf
5
s
s
stf
c
6
ap
s
s
ss
sg
c

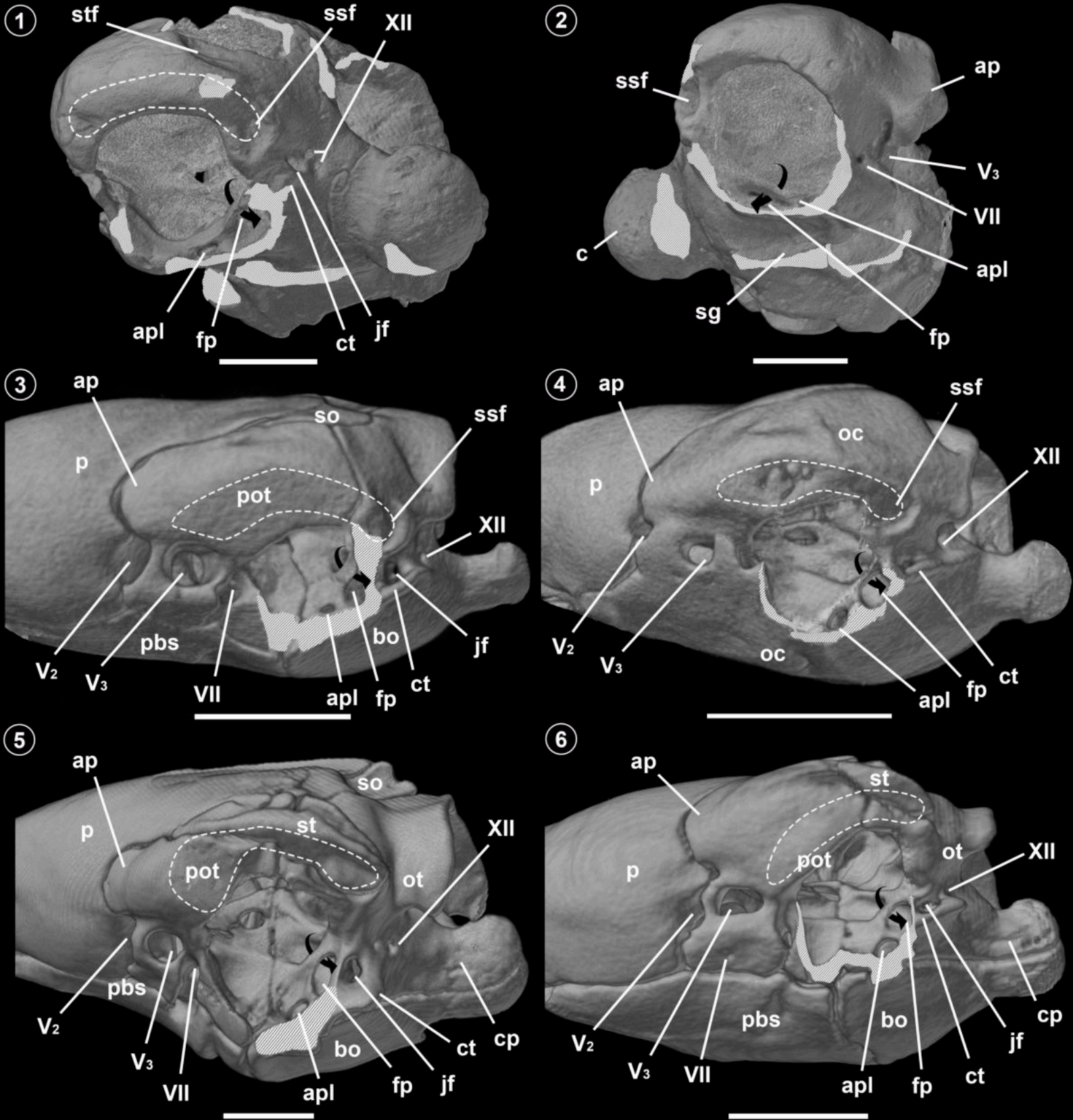
1
stf
ssf
XII
apl
fp
ct
jf
2
ap
ssf
V3
VII
apl
c
sg
fp
3
ap
so
ssf
p
pot
XII
V2
V3
pbs
VII
apl
fp
bo
ct
jf
4
ap
ssf
oc
XII
p
V2
V3
oc
apl
fp
ct
5
ap
so
p
st
XII
pot
ot
pbs
V2
V3
VII
apl
bo
fp
jf
ct
cp
6
ap
st
p
pot
ot
XII
V2
V3
VII
pbs
apl
bo
fp
ct
jf
cp

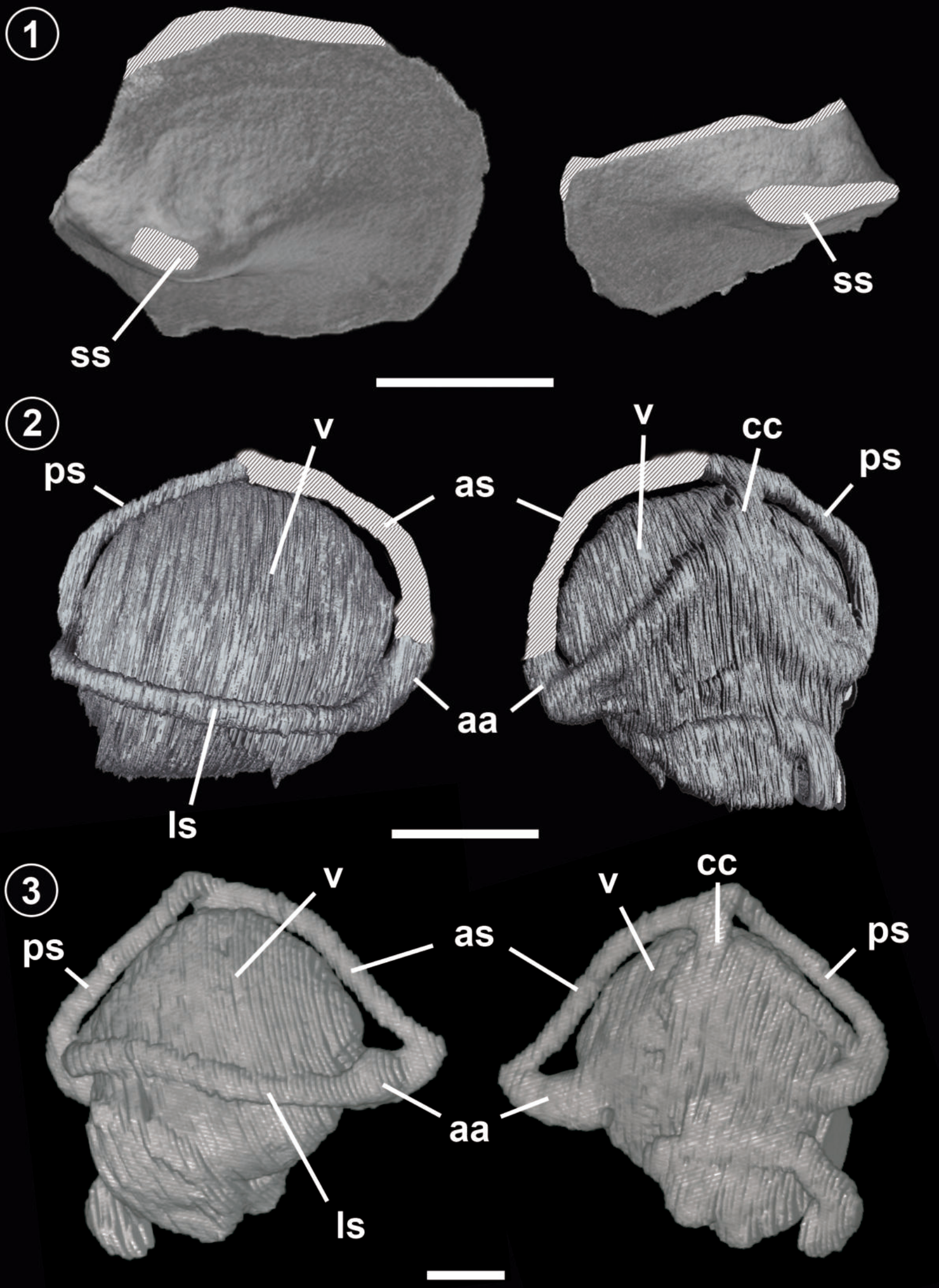
1
ss
ss
2
ps
v
as
aa
ls
v
cc
ps
3
ps
v
as
aa
ls
v
cc
ps

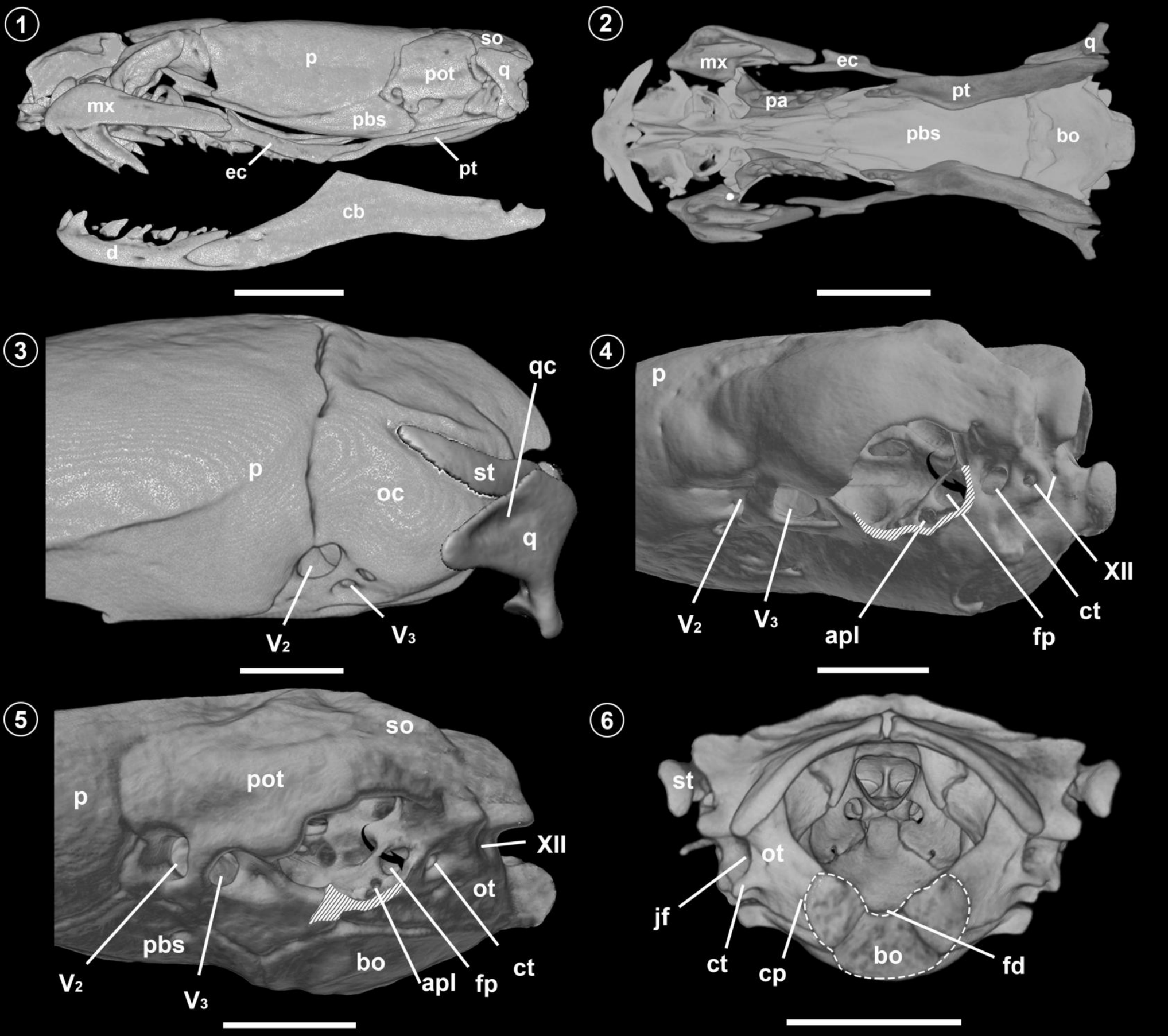
1
so
p
pot
q
mx
pbs
ec
pt
cb
d
2
q
mx
ec
pt
pa
pbs
bo
3
qc
p
st
oc
q
V2
V3
4
p
V2
V3
apl
fp
ct
XII
5
so
pot
p
XII
ot
pbs
bo
V2
V3
apl
fp
ct
6
st
ot
jf
ct
cp
bo
fd

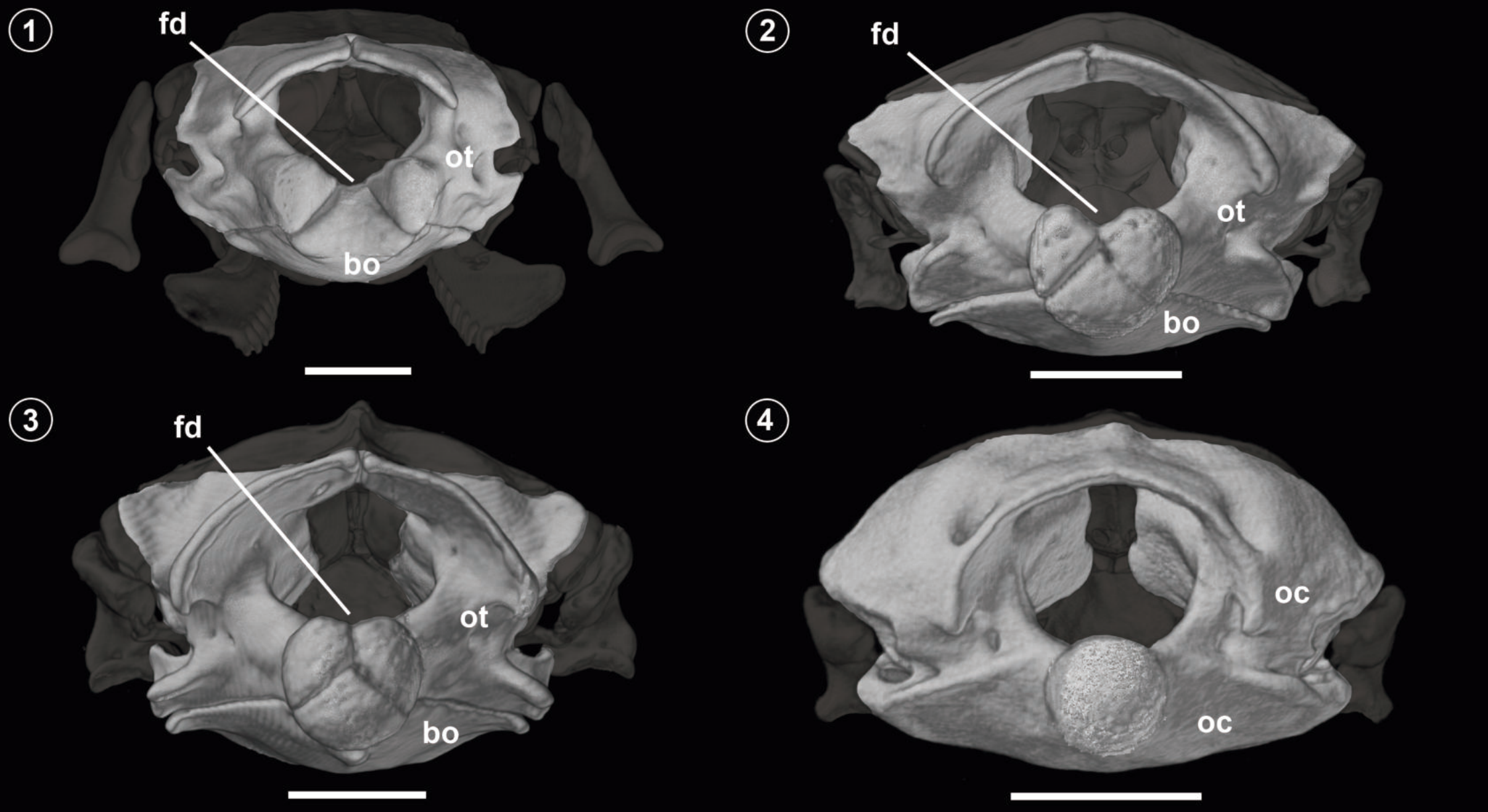
1
fd
ot
bo
2
fd
ot
bo
3
fd
ot
bo
4
oc
oc

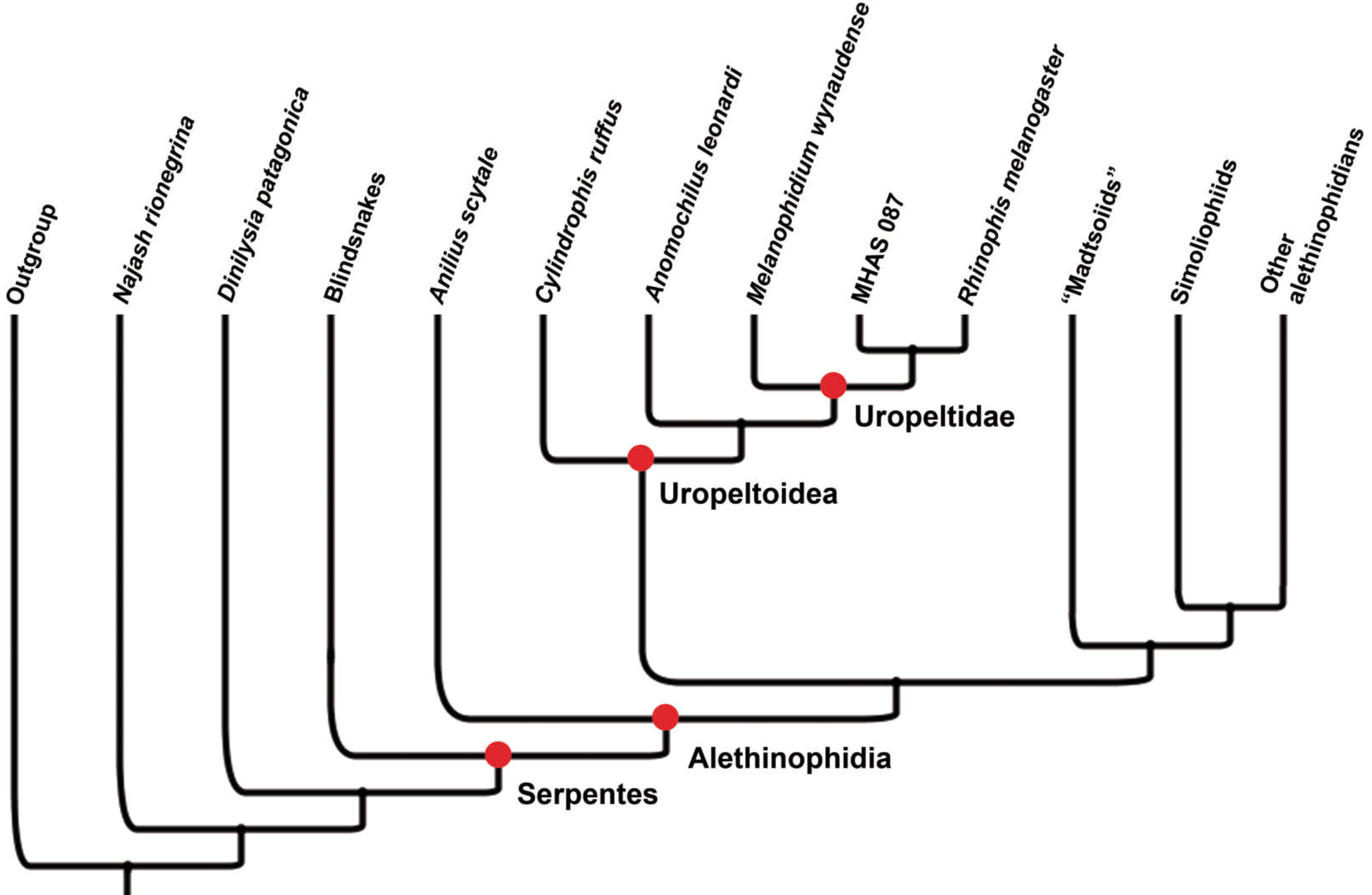
Outgroup
Najash rionegrina
Dinilysia patagonica
Blindsnakes
Anilius scytale
Cylindrophis ruffus
Anomochilus leonardi
Melanophidium wynaudense
MHAS 087
Rhinophis melanogaster
"Madtsoiids"
Simoliophiids
Other alethinophidians
Uropeltidae
Uropeltoidea
Alethinophidia
Serpentes